Gravitational and Dynamic Components of Muscle Torque Underlie Tonic and Phasic Muscle Activity during Goal-Directed Reaching

Erienne V. Olesh [1,2], Bradley S. Pollard [1,2] and Valeriya Gritsenko [1,2,3*]

[1] Department of Human Performance, School of Medicine, West Virginia University, Morgantown, WV, United States, [2] Centers for Neuroscience, School of Medicine, West Virginia University, Morgantown, WV, United States, [3] Department of Mechanical and Aerospace Engineering, Benjamin M. Statler College of Engineering and Mineral Resources, West Virginia University, Morgantown, WV, United States

Human reaching movements require complex muscle activations to produce the forces necessary to move the limb in a controlled manner. How gravity and the complex kinetic properties of the limb contribute to the generation of the muscle activation pattern by the central nervous system (CNS) is a long-standing and controversial question in neuroscience. To tackle this issue, muscle activity is often subdivided into static and phasic components. The former corresponds to posture maintenance and transitions between postures. The latter corresponds to active movement production and the compensation for the kinetic properties of the limb. In the present study, we improved the methodology for this subdivision of muscle activity into static and phasic components by relating them to joint torques. Ten healthy subjects pointed in virtual reality to visual targets arranged to create a standard center-out reaching task in three dimensions. Muscle activity and motion capture data were synchronously collected during the movements. The motion capture data were used to calculate postural and dynamic components of active muscle torques using a dynamic model of the arm with 5 degrees of freedom. Principal Component Analysis (PCA) was then applied to muscle activity and the torque components, separately, to reduce the dimensionality of the data. Muscle activity was also reconstructed from gravitational and dynamic torque components. Results show that the postural and dynamic components of muscle torque represent a significant amount of variance in muscle activity. This method could be used to define static and phasic components of muscle activity using muscle torques.

Keywords: EMG, principal component analysis, kinematics and dynamics, motor systems and movement control, arm

INTRODUCTION

The musculoskeletal anatomy of the body constitutes a complex dynamical system that is a challenge to control for the central nervous system (CNS). Some of the complexity is due to the muscular redundancies that allow humans to perform complex tasks. Additional complexity results from the forces associated with the mechanical properties of the multi-joint limb, termed

limb dynamics. How the CNS deals with limb dynamics is commonly investigated through joint torques, or rotational forces, that arise during motion of the limb (Flanders, 1991; Sainburg et al., 1995, 1999; Shabbott and Sainburg, 2008) or from action of external forces when the limb is held stationary (Buneo et al., 1997; Weiss and Flanders, 2004). During these tasks, angular kinematics (position and velocity) can be used to derive joint torques for each independent direction of motion termed degree of freedom (DOF) using equations of motion. The goal is to derive the active torques that are the result of muscle contractions in the presence of passive forces that have both extrinsic and intrinsic sources (Papaxanthis et al., 2005; Gentili et al., 2007; Le Seac'h and McIntyre, 2007; Dounskaia and Wang, 2014). A large contributor to the extrinsic passive torques is gravity. These gravitational torques depend on the orientation of limb segments in space, and thus they contribute to both posture and movement (Bastian et al., 1996). The compensation for gravitational torques is important for motor control, as evidenced by altered patterns of movement errors and muscle activity of people moving in micro-gravity environments (Fisk et al., 1993; Papaxanthis et al., 1998, 2005; Pozzo et al., 1998). Gravity torques can also be optimally integrated in the planning of rapid arm movements and exploited to reduce muscular efforts during rapid motions (Gaveau et al., 2014, 2016; Rousseau et al., 2016). Studies of cerebella pathologies and adaptation after returning from microgravity environment to normal gravity have also suggested that the effect of gravity on the arm may be separately estimated from the effect of dynamic torques (Gaveau et al., 2011; Sajdel-Sulkowska, 2013). The proportion of active muscle torques that is responsible for gravity compensation can be estimated as the difference between muscle torques produced in a micro-gravity environment and muscle torques produced under normal gravity. This portion of muscle torques has a different temporal profile than that of the motion-related dynamic components of muscle torque (Russo et al., 2014). In another definition, the dynamic component of muscle toque varies with the speed of movement, while the gravitational component of muscle torque does not (Hollerbach and Flash, 1982; Flanders and Herrmann, 1992). In this study, we obtain both dynamic and gravitational components of muscle torque produced during pointing in virtual reality by healthy human subjects.

Traditionally, the postural transition component of muscle activity has been estimated as a linear ramp in electromyography (EMG) during movement. The ramp is calculated between EMG values obtained before and after movement, i.e., during posture maintenance (Buneo et al., 1994; Flanders et al., 1996). This static component is often subtracted from the EMG during movement, and the residual phasic EMG is studied as the motion-related signal. While the estimate of postural EMG are valid, there is no physiological evidence for a linearly-changing EMG associated with the transition between postures during movement. An improvement on this technique would be a quantitative estimate of the contribution of gravity acting on the limb during movement to muscle activity. In addition, relating phasic EMG to the dynamic component of muscle torque would be useful in evaluating the contribution of individual muscles to

active torques responsible for movement vs. joint stiffness, that is not accounted for by active torques. Damage to the cerebellum appears to uniquely affect the phasic component of EMG in a way that supports its role in controlling passive torques (Manto and Bosse, 2003). The rationale of this study was to contribute a new method for dividing the EMG into static and phasic components by evaluating the different contribution of torque components to the overall EMG. EMG of different muscles and torques about different DOFs are coupled through the kinematic chain of the limb. We control for this coupling by reducing the dimensionality of our data using principal component analysis (PCA). We use PCA to obtain independent components from muscle torques and compare them to the independent components obtained from EMG. We also calculate the amount of variance that the gravitational and dynamic components of muscle torque account for in EMG. We expect that gravitational and dynamic torque components capture significant amounts of variance in EMG and their waveforms can be used to identify static and phasic components in EMG.

METHODS

Ten healthy individuals (7 males, 3 females) with an average age of 26 ± 11 years old were recruited to perform
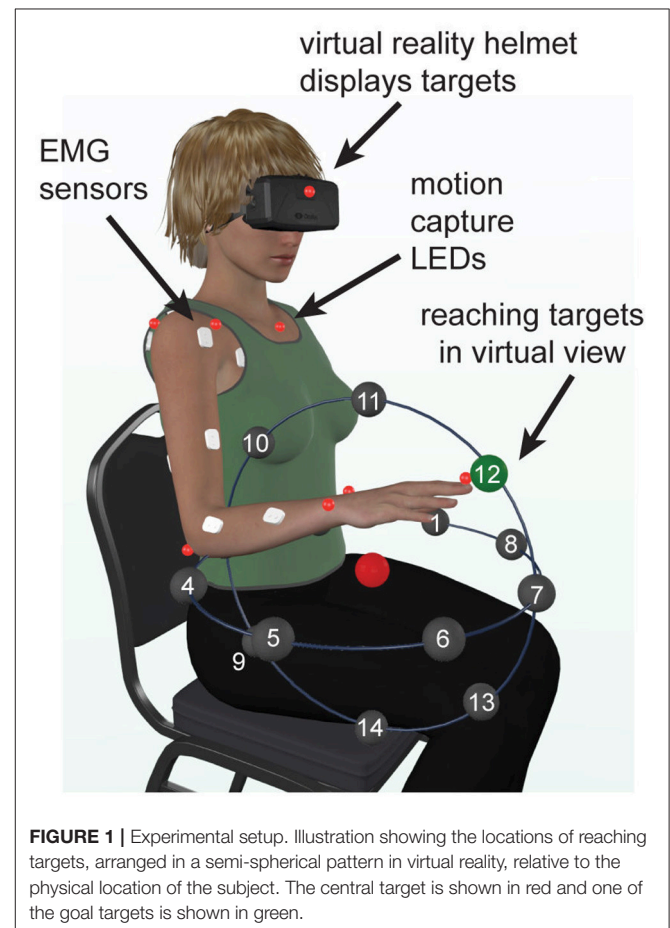

FIGURE 1 | Experimental setup. Illustration showing the locations of reaching targets, arranged in a semi-spherical pattern in virtual reality, relative to the physical location of the subject. The central target is shown in red and one of the goal targets is shown in green.

a reaching "center-out" task. The study and the consent procedure were approved by the Institutional Review Board of West Virginia University (Protocol # 1311129283). All subjects provided their written consent prior to participating in the study. All subjects were right-hand dominant and reported no movement disorders and no major injuries to their right arm. Height, weight, and arm segment lengths were measured for each subject and used to adjust model parameters to create subject-specific dynamic models (see below).

Movements were instrumented using a virtual reality (VR) software (Vizard by Wolrdviz) and head set (Oculus Rift), which displayed 14 targets arranged in two perpendicular planes, horizontal transverse plane and vertical coronal plane (**Figure 1**). To reduce inter-subject variability in kinematic data, the target locations were adjusted for each subject based on the lengths of their arm segments, which ensured the same initial and final joint angles across all subjects. The center target was placed so that initial arm posture was at 0° shoulder flexion, 90° elbow flexion, and a 0° wrist flexion. The distance from the center target to the peripheral targets was scaled to 30% of each subject's total arm length (from anterior acromial point to the distal end of the index finger). On average, this amounted to 20 cm distance from the central to peripheral targets. This scaling reduced the inter-subject variability in the joint angles at each peripheral target. Each movement began with the subject pointing to the center target, which was the only one visible. After VR detected the tip of the subject's finger inside the target radius, the central target changed color and one peripheral target appeared. When the VR detected the tip of the subject's finger inside the peripheral target radius, it changed color, which cued the subject to return to the central target. Upon returning to the central target the task reset, peripheral target disappeared and a new one appeared after a delay of 0.5 s. Subjects were instructed to not move the trunk, keep their wrist pronated and straight, and point as quickly and accurately as possible. Movements to each target location were repeated 15 times and performed in a randomized order.

Arm and trunk movements were recorded with an active motion capture system (PhaseSpace, Impulse) at 480 frames per second. The light emitting diodes of the motion capture system were placed on anatomical landmarks according to best practice guidelines (Robertson et al., 2013) EMG was recorded from 12 arm muscles at a rate of 2,000 Hz (MA400-28 MotionLab Systems). Muscles recorded during the experiment included the pectoralis major (Pec), teres major (TrM), anterior deltoid (AD), posterior deltoid (PD), long and short heads of the biceps (BiL and BiS respectively), lateral and long heads of the triceps (TrLa and TrLo respectively), brachioradialis (Br), flexor carpi ulnaris (FCU), flexor carpi radialis (FCR), and extensor carpi radialis (ECR). Motion capture and EMG were synchronized using a custom circuit and triggering mechanism (Talkington et al., 2015). Motion capture and EMG data were imported into Matlab and processed as follows using custom scripts.

Digitized EMG data were high pass filtered at 20 Hz to remove motion artifacts, rectified, and low pass filtered at 10 Hz, consistent with SENIAM recommendations. Motion capture data

were low pass filtered at 10 Hz and interpolated with a cubic-spline. The maximum interpolated gap was 0.2 s. The onset and offset of movement was found based on the velocity of three hand LEDs changing by five percent of the maximum velocity for a given movement. These events were used for temporal normalization of all data. Signals starting 200 ms prior to the onset of movement were included in all analyses to ensure adequate capture of initial EMG bursts and onset of phase-advanced torques. Arm kinematics were obtained from motion capture by fitting local coordinate systems to form rigid bodies from markers for the trunk, upper arm, forearm, and hand. The axes of these coordinate systems were oriented so that X/Y plane matched the frontal plane of the body with Y pointing along the long axis of each segment opposite to the gravity vector; Z was completing the right-handed basis. The Euler angles between these local coordinate systems in time were obtained using linear algebra for five joint DOFs including shoulder (flexion/extension, abduction/adduction, pronation/supination), elbow (flexion/extension), and wrist (flexion/extension). The posture with 0 angles corresponded to the arm straight along the body with hand pronated. Angular velocity and acceleration were calculated by differentiating the Euler angles waveforms. Hand pronation/supination and wrist abduction/adduction were found to be minimal during the pointing task, and thus these DOFs were not included in the analysis.

Limb Dynamics

To calculate joint torques, an inverse dynamic model of the subject's arm was constructed in Simulink (MathWorks). The model comprised 5 DOFs as described above and three segments approximating inertial properties of the arm, forearm, and hand. Motion of the trunk was found to be minimal during the task, thus the model had the trunk fixed in space. Inertia of the segments was approximated with a cylinder of the length equal to that of the corresponding segment and a 3 cm radius. The masses and centers of mass for each segment were determined by their anthropometric ratios to the subjects' segment lengths and weight (Winter, 2009). The model implemented equations of motion that can be summarized as follows:

$$\tau_N = \tau_M + \tau_{IT} + \tau_G \qquad (1)$$

where τ_N is a vector of net torques that produce movement; τ_M is a vector of active torques due to muscle contractions; τ_{IT} is a vector of passive interaction torques; τ_G is a vector of passive torques caused by gravity.

Angular kinematics averaged per movement direction and per subject was used in the subject-specific inverse model to calculate muscle torques, similar to that in Russo et al. (2014). This is equivalent to rearranging the Equation (1) as follows:

$$\tau_M = \tau_N - \tau_{IT} - \tau_G \qquad (2)$$

The computed muscle torques are proportional to the sum of all moments generated by muscles spanning the joints:

$$\tau_M = \sum_{i=1}^{N} R_i \times A_i \qquad (3)$$

where R_i is moment arm of muscle i about a given DOF, and A_i is activation of muscle i. The numerical quality of inverse dynamic simulations was checked by running the same model in forward dynamics mode using the calculated torques as inputs and simulated angular kinematics as outputs. The simulated and experimental joint kinematics was compared, and the mean $\pm$ standard deviation of the root-mean-squared differences between them was 0.05 ± 0.02 radians across all DOFs.

As described in the Introduction, muscle activity is often separated into static and phasic components. Here we propose to use the gravitational and dynamic components of muscle torque to define the static and phasic components of EMG respectively. This can be represented as follows:

$$A_i = D_i + G_i \qquad (4)$$

and substituting Equation (4) into (3) gives,

$$\tau_M = \sum_{i=1}^{N} R_i \times D_i + \sum_{i=1}^{N} R_i \times G_i \qquad (5)$$

Because torques are additive, the muscle torques obtained using the inverse model can be separated into two components (Gottlieb et al., 1997; Russo et al., 2014) as described in the Introduction above. To estimate the dynamic component of muscle torques responsible for motion production and inter-joint coordination without gravity, the inverse model was run without simulating external gravitational force (the parameter for gravitational force in the physics engine was set to 0). This resulted in the following:

$$\tau_{MD} = \tau_N - \tau_{IT} \qquad (6)$$

where τ_{MD} are muscle torques that would produce the same motion without gravity as that recorded in the presence of gravity. Example of such torques would be the sum of muscle moments produced during motion in microgravity environment. Another example are torques necessary for planar movements in a horizontal plane, where the force of gravity is perpendicular to the plane of motion (Debicki and Gribble, 2005). Then the component of muscle torque that is needed to compensate for gravity (τ_{MG}) can be estimated as the difference between muscle torques with and without gravity as follows:

$$\tau_{MG} = \tau_M - \tau_{MD}, \text{or}$$
$$\tau_M = \tau_{MD} + \tau_{MG} \qquad (7)$$

Below, τ_{MD} is referred to as MD torque, while τ_{MG} is referred to MG torque for simplicity.

The relative contribution of MG and MD torques to the overall muscle torques τ_M based on Equation (7) was calculated as the shared variance between each torque component and muscle torque for a corresponding DOF. The coefficient of determination (r^2) was used to quantify shared variance between MG and muscle torques and separately between MD and muscle torques for corresponding DOFs per movement direction per subject.

Dimensionality Reduction

To control for widespread correlations between biological signals, EMG and dynamic data were reduced in dimensionality using PCA. Rectified EMG signals were normalized to movement duration, averaged per movement direction, and low pass filtered at 10 Hz. To ensure that muscle activations were unitless, maximum contraction values were calculated for each muscle across all movement directions and used to divide mean EMG for each movement direction. The resulting data matrix was comprised of 336 columns (12 EMG signals for 14 movements toward each virtual target and 14 return movements) and 1000 rows representing samples in time. To ensure that MD and MG torques were unitless, the maximal amplitudes across all movement directions were used to divide torques for each movement direction. The MD and MG torque data matrices were comprised of 140 columns each (torques for 5 DOFs for 14 movements toward each virtual target and 14 return movements) and 1000 rows representing samples in time. All data were demeaned; eigenvalues and eigenvectors were obtained using singular value decomposition in Matlab. Eigenvectors were direction independent waveforms in time, while eigenvalues represented projections of signals onto the eigenvectors per muscle or DOF per movement direction.

To evaluate the contribution of gravity and dynamic torques to muscle activation, the first eigenvectors that captured the most variance in MD and MG data were used to decompose EMG data. Projections of EMG data onto the torque eigenvectors, the z-scores, were calculated using dot product. The EMG data were then reconstructed back from the obtained z-scores and torque eigenvectors. The coefficient of determination (r^2) was used to quantify the quality of EMG reconstruction. Separate r^2 were calculated to evaluate the amount of shared variance captured by each of the torque eigenvectors.
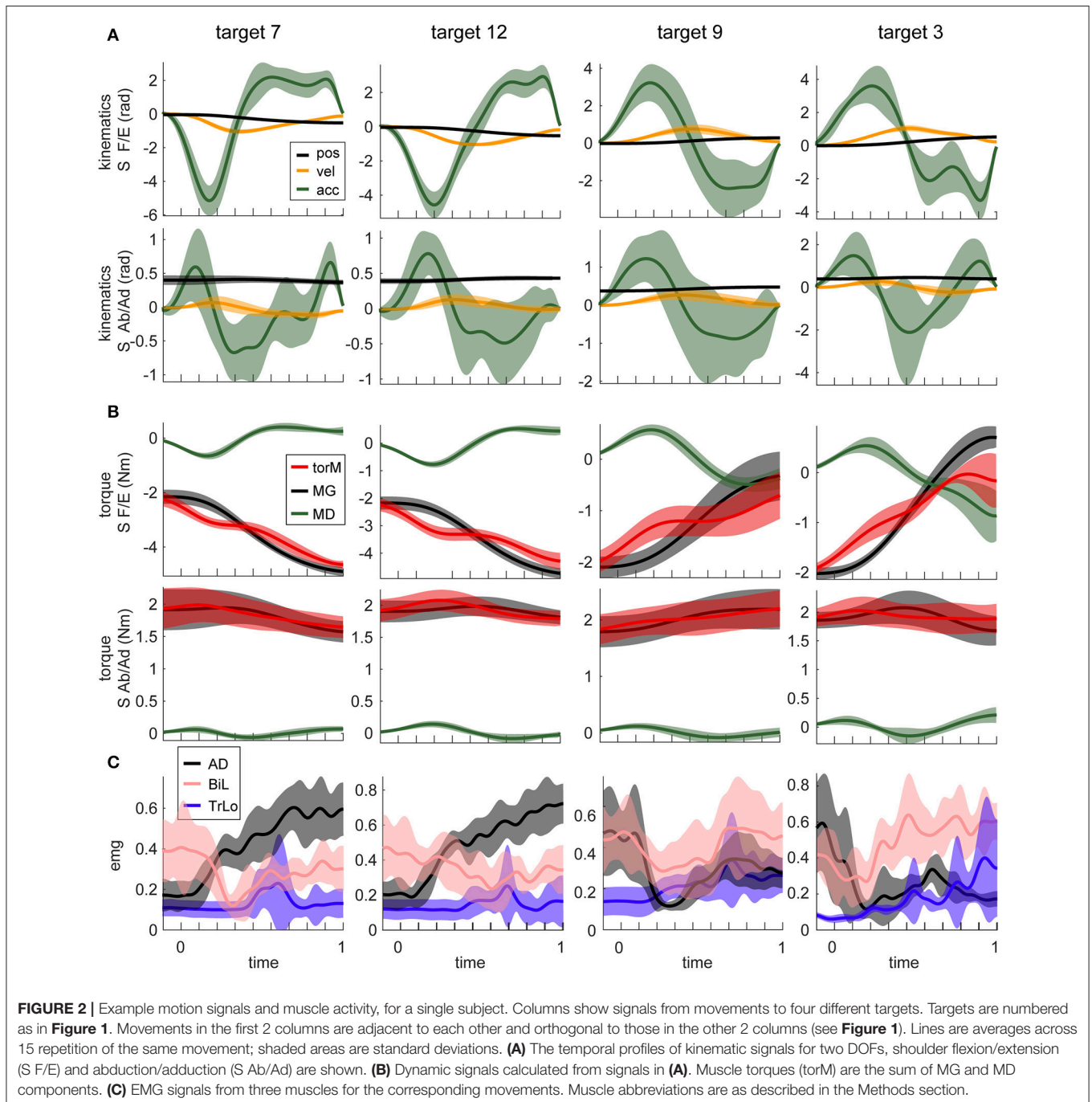
Statistical Analysis

Statistics on r^2-values was done using repeated measures analysis of variance (rANOVA) in MATLAB. A single rANOVA model was fitted to the r^2 from EMG decomposition and the r^2 from torque components across all signals and movement directions per subject. The model utilized a within-subject design with three factors. The first factor grouped data based on torque (PCA eigenvalues) or muscle (EMG decomposition z-scores). The second factor grouped data based on the type of component (dynamic or gravitational). The movement factor grouped data based on the direction of movement (14 unique directions in **Figure 1**). *Post-hoc* multiple comparisons were used to further examine significant interactions. Linear regressions between the r^2 from EMG decomposition and the r^2 from torque components were used as measures of the contribution of MG and MD torques to EMG. The rANOVA was also repeated on r^2-values for only active EMG signals, for which the peak of mean EMG activity was >30% of maximal peak across movement directions.

Data trends are reported using means $\pm$ standard deviations across subjects, which are included in the Results section below unless otherwise specified.

RESULTS

The motion in virtual reality was highly consistent, as demonstrated by the low standard deviations of angular kinematics across the 15 repetitions of each movement (**Figure 2A**). The mean endpoint error was 0.04 ± 0.01 m across subjects. The kinematic profiles showed typical motor invariance with bell-shape velocity profiles with peaks ranging from 1.2 to 3.3 m per second, and accompanying acceleration

and deceleration phases (**Figure 2A**). The movements were produced by active muscle torques, whose temporal profiles were subdivided into gravitational MG and dynamic MD components as described in the Methods (**Figure 2B**). The MG component waveform changed in a single direction during a given movement and was the source of the offset in the muscle torque waveforms. The waveform of the MD component was largely similar to the angular acceleration waveform. As expected, muscle activity was more variable across subjects, but most muscles did follow a

FIGURE 2 | Example motion signals and muscle activity, for a single subject. Columns show signals from movements to four different targets. Targets are numbered as in **Figure 1**. Movements in the first 2 columns are adjacent to each other and orthogonal to those in the other 2 columns (see **Figure 1**). Lines are averages across 15 repetition of the same movement; shaded areas are standard deviations. **(A)** The temporal profiles of kinematic signals for two DOFs, shoulder flexion/extension (S F/E) and abduction/adduction (S Ab/Ad) are shown. **(B)** Dynamic signals calculated from signals in **(A)**. Muscle torques (torM) are the sum of MG and MD components. **(C)** EMG signals from three muscles for the corresponding movements. Muscle abbreviations are as described in the Methods section.

reciprocal pattern of activation for movements in the opposite directions (**Figure 2C**, first 2 columns vs. the last 2 columns).

The linear dependencies across torque components and across EMGs were examined using PCA as described in Methods. In MG torques across all movements, a single principal component accounted for 96 ± 1% of variance. The second principal component accounted for 4 ± 1% of variance, and the rest accounted for progressively less variance. For MD torques across all movements, a single principal component accounted for 92 ± 2% of variance. The second principal components accounted for 6 ± 2% of variance. In contrast, for EMG the first three principal components accounted for a comparable amount of total variance, 72 ± 6%, 12 ± 3%, and 5 ± 2% of variance accounted for by the principal components 1 through 3, respectively. The waveforms (eigenvectors) of the first and second principal components of EMG were very similar to the first principal components of MG and MD torques, respectively (**Figure 3A**). Therefore, we used the first principal components of MG and MD torques to decompose EMG data and calculate the variance accounted for by these dynamic signals.

The total variance accounted for by torque decomposition of EMG was 55 ± 10% across subjects. Analysis of a subset of variances for only active EMGs (see Methods) increased the total variance accounted for by torque decomposition of EMG to 65 ± 15% across subjects. For individual muscles, the total and relative variances accounted for by torque components was largely the same (**Figure 4**). The relative variance in EMG accounted for by each torque principal component was lower than the relative variance that MG and MD torques contribute to the muscle torque (rANOVA: difference = 21%; standard error = 1%; $p <$ 0.001). Analysis of a subset for active EMGs showed a decreased difference (rANOVA: difference = 12%; standard error = 3%; p = 0.008). The dynamic principal component accounted for less variance in EMG than expected from MD contribution to muscle torque (rANOVA: difference = 26%; standard error = 1%; p < 0.001) and the gravitational component accounted for less variance in EMG than expected from MG contribution to muscle torque (rANOVA: difference = 16%; standard error = 2%; $p <$ 0.001). Analysis of a subset for active EMGs showed decreased differences in both cases (rANOVA on MD vs. dynamic EMG: difference = 19%; standard error = 3%; p = 0.005) compared to those for gravitational components (rANOVA on MG vs. gravitational EMG: difference = 6%; standard error = 2%; p = 0.069). There was no average difference between the relative contributions of the gravitational and dynamic components across all movement and signals (rANOVA: difference = 5%; standard error = 1%; p = 0.628).

As expected, the eigenvalues from torque PCA and z-scores from EMG decomposition were directionally tuned (Supplementary Figure). Consequently, the total variance accounted for by torque decomposition of EMG varied across movement directions (**Figure 5A**). The relative contribution of gravitational component to EMG varied independently from the relative contribution of MG component to muscle torque across the different movement directions (**Figure 5B**). There was an insignificant correlation between the mean contribution of
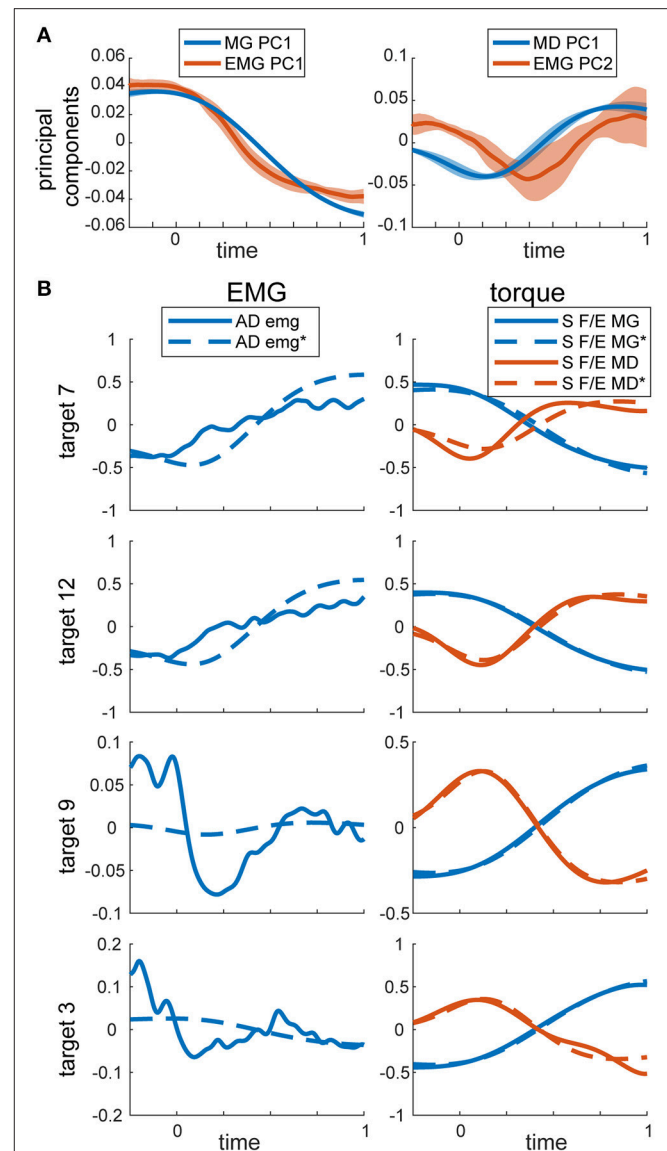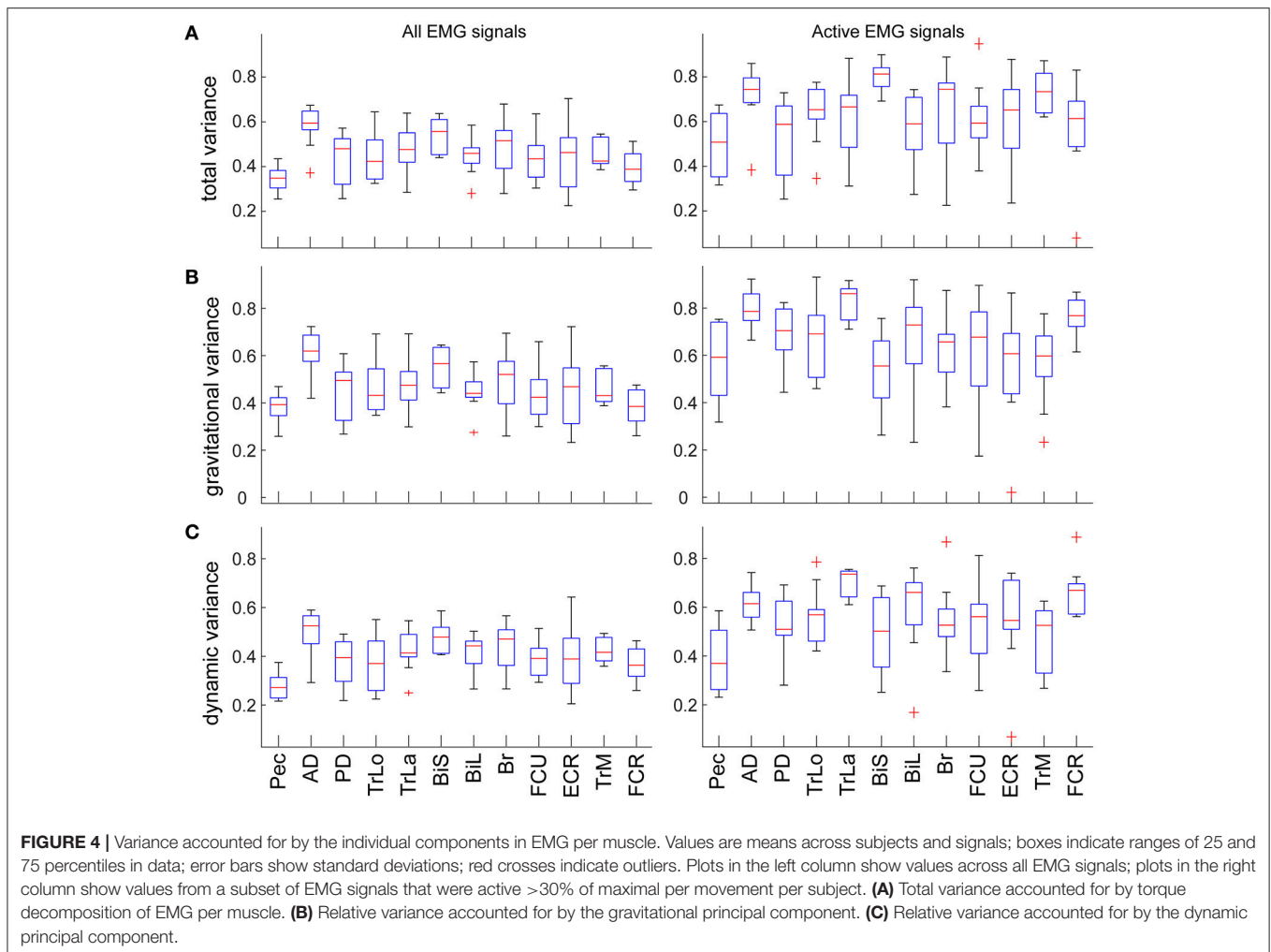

FIGURE 3 | PCA on torques and EMG. **(A)** Temporal activation profiles of EMG and torque components. Average normalized activation profiles (solid lines) and standard deviations (shaded area) across all subjects are plotted for each eigenvector. **(B)** Example recorded and reconstructed signals from the same subject and movements as in **Figure 2**. MG and MD torques were reconstructed from their respective first principal components only. EMG was reconstructed from the same torque components as described in Methods. MG and MD torques and EMG were normalized and demeaned as described in Methods. Reconstructed signals are labeled with * and marked with dashed lines. S F/E stands for Shoulder flexion/extension torque.

gravitational component to EMG and MG to muscle torque (Pearson correlation coefficient $r = -0.07$, $p = 0.812$). At the same time, the relative contributions of both gravitational and dynamic components to EMG were inversely correlated with the contribution of MD to muscle torque (**Figure 5C**; $r = -0.56$, $p = 0.039$ for gravitational EMG component and MD; $r = -0.62$, $p = 0.018$ for dynamic EMG component and MD). There was also an
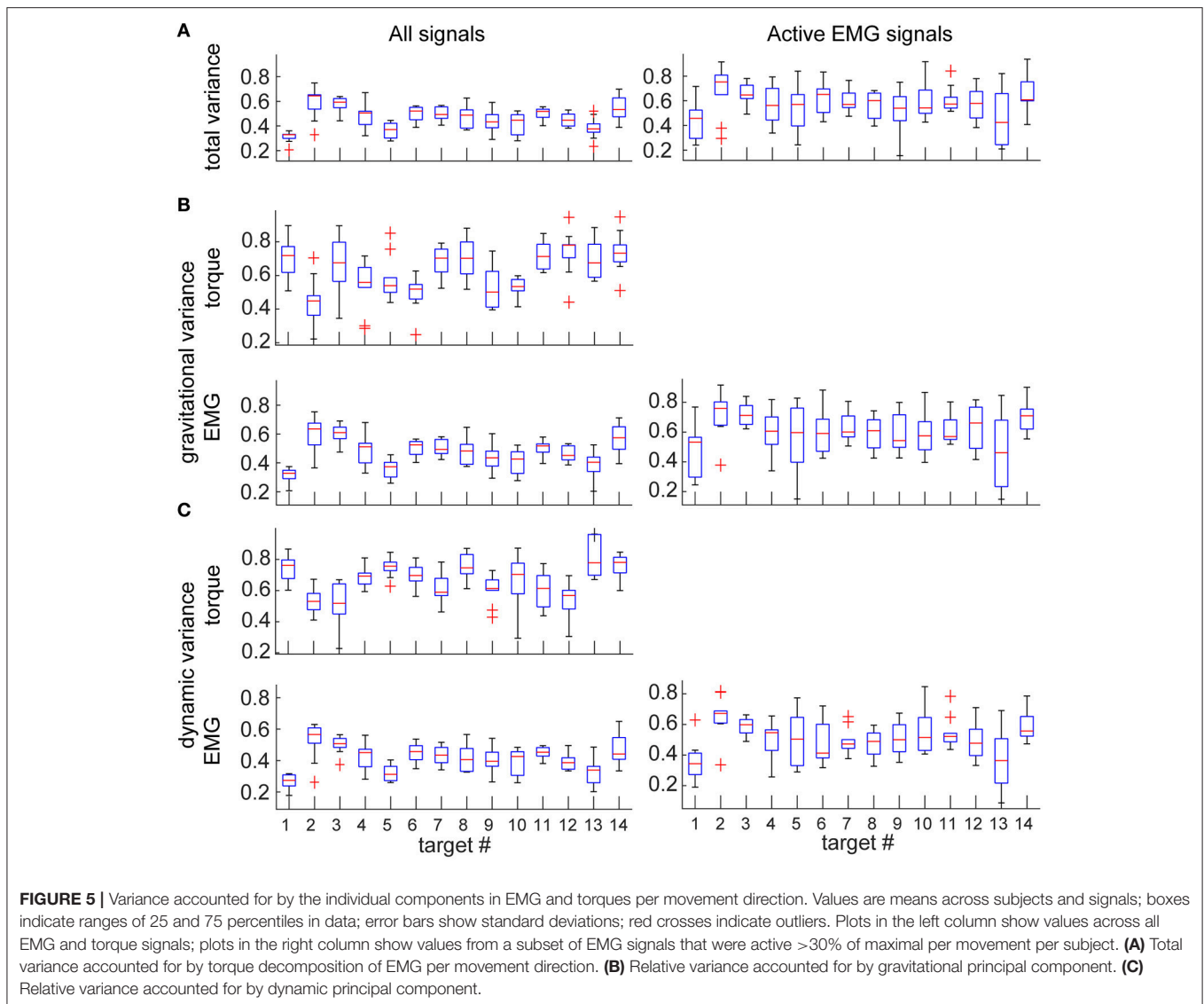
FIGURE 4 | Variance accounted for by the individual components in EMG per muscle. Values are means across subjects and signals; boxes indicate ranges of 25 and 75 percentiles in data; error bars show standard deviations; red crosses indicate outliers. Plots in the left column show values across all EMG signals; plots in the right column show values from a subset of EMG signals that were active >30% of maximal per movement per subject. **(A)** Total variance accounted for by torque decomposition of EMG per muscle. **(B)** Relative variance accounted for by the gravitational principal component. **(C)** Relative variance accounted for by the dynamic principal component.

inverse correlation between the total variance accounted for by torque decomposition of EMG and MD contribution to muscle torque ($r = -0.58$, $p = 0.028$).

For movements in different directions, the muscle torques are accompanied by different amounts of relative contribution from MG and MD torques. We found that there were many instances, in which one or the other torque component tended to dominate the overall muscle torque, which is reflected in a distribution of r^2-values along the maximal and minimal values (**Figure 6**, blue). However, this was not the case for the distribution of r^2-values for the contributions of torque principal components to EMG (**Figure 6**, red). Surprisingly, the relative contributions of both torque principal components to EMG varied together in all muscles across all movement directions. This relationship was well fitted with a linear regression ($p < 0.001$ for all subjects), the slopes of these regressions ranged from 0.66 to 0.87 across subjects. This linear relationship between the contributions of the gravitational and dynamic torque principal components to EMG across all subjects was also present when only active EMG signals per movement per subject were selected (**Figure 7**).

DISCUSSION

The transformation from muscle activation to motion is non-linear and includes at least second order differential dynamics. The transformation includes non-linear muscle properties and Newton-Euler equations of motion (Winter, 2009). This dynamics is often thought to be imbedded by the CNS either in the forms of internal models (Lackner and Dizio, 1994; Shadmehr and Mussa Ivaldi, 1994; Gomi and Kawato, 1997; Wolpert and Kawato, 1998; Sabes, 2000) or neural primitives (or synergies) (Bizzi et al., 1991; Giszter et al., 1993; Mussa Ivaldi, 1999; Mussa Ivaldi and Bizzi, 2000; for a review see d'Avella and Lacquaniti, 2013). Here, we do not try to resolve the problem of whether the control has two components, static and dynamic. Instead, we used the causal relationship between muscle contraction and motion to investigate how limb dynamics is reflected in muscle activity. We have demonstrated a method to compute phasic and tonic components of EMG using muscle torques. We have found that these components capture on average 55% of variance in EMG signals. Although there is no novelty in a general statement that gravity influences control signals, our novel result is the

FIGURE 5 | Variance accounted for by the individual components in EMG and torques per movement direction. Values are means across subjects and signals; boxes indicate ranges of 25 and 75 percentiles in data; error bars show standard deviations; red crosses indicate outliers. Plots in the left column show values across all EMG and torque signals; plots in the right column show values from a subset of EMG signals that were active >30% of maximal per movement per subject. **(A)** Total variance accounted for by torque decomposition of EMG per movement direction. **(B)** Relative variance accounted for by gravitational principal component. **(C)** Relative variance accounted for by dynamic principal component.

quantitative measure of the amount of EMG variance captured by gravitational and dynamic components of muscle torques. No other study reported that. We will discuss our results within a context of a general control schema that combines multiple views on the organization of the motor control system (**Figure 8**).

The similarities in the waveforms of dynamic torques across DOFs and movements have been previously reported and interpreted as evidence of central planning (Hollerbach and Flash, 1982; Gottlieb et al., 1997; Thomas et al., 2005). Here we also show that a single principal component accounts for most of the variance in MD and MG torque waveforms. Similar single principal components were reported to capture most of the variance in kinematics and in dynamic torques during whole body reaching movements (Thomas et al., 2005). Although, our results show that the kinematic waveform in the Thomas et al. (2005) study may also be consistent with the gravitational torque waveform. Our results further show that

the gravitational and dynamic components of muscle torque explain on average 55% of EMG waveforms during goal-directed reaching movements, with slightly more variance accounted for by the gravitational component than the dynamic component in active muscles. This is further supported by the similarity between the first 2 principal components obtained from EMG and the first principal components obtained from gravitational and dynamic torque components separately (**Figure 3**). This is consistent with previous work showing that the first two principal components in EMG are related to static and phasic components of EMG waveforms (Flanders and Herrmann, 1992). Thus, the hypothetical neural control signals originating in the supraspinal structures of the CNS and then combining at the spinal level with sensory feedback may consist of two commands, a gravitational and a dynamic command (**Figure 8**). These commands could then underlie phasic and tonic components of EMG (Flanders, 1991; d'Avella et al., 2008). The supraspinal command that
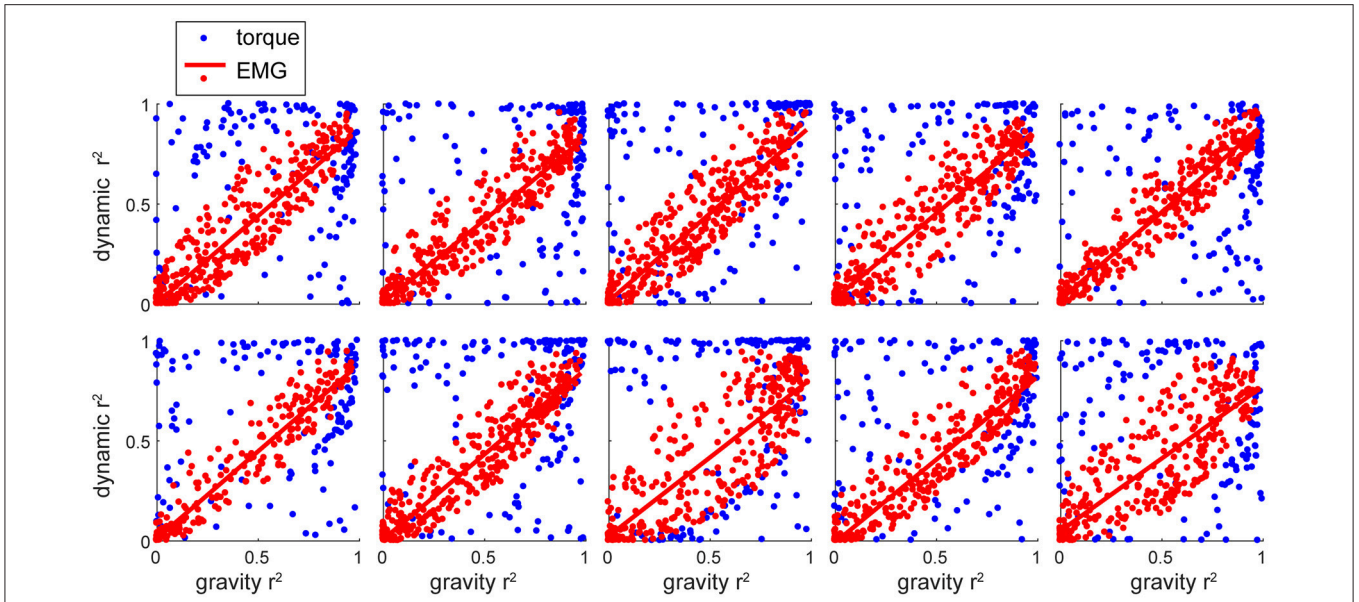
FIGURE 6 | The relative contribution of individual components to EMG and muscle torques per subject. Each plot shows data for a single subject. Each dot represents a value per signal (muscle or DOF) per movement.
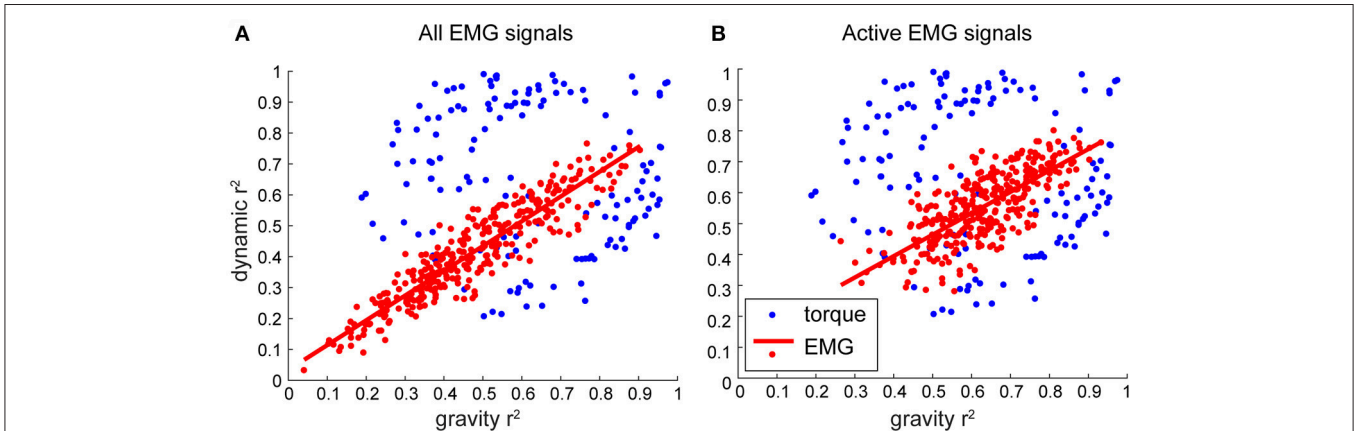

FIGURE 7 | The relative contribution of individual components to EMG and muscle torques across subjects. Each dot represents a value per subject per movement averaged across signals/DOFs. **(A)** Combined data across subjects. **(B)** Combined data across subjects, where only variance for conditions when EMG was active >30% of maximal was selected before averaging.
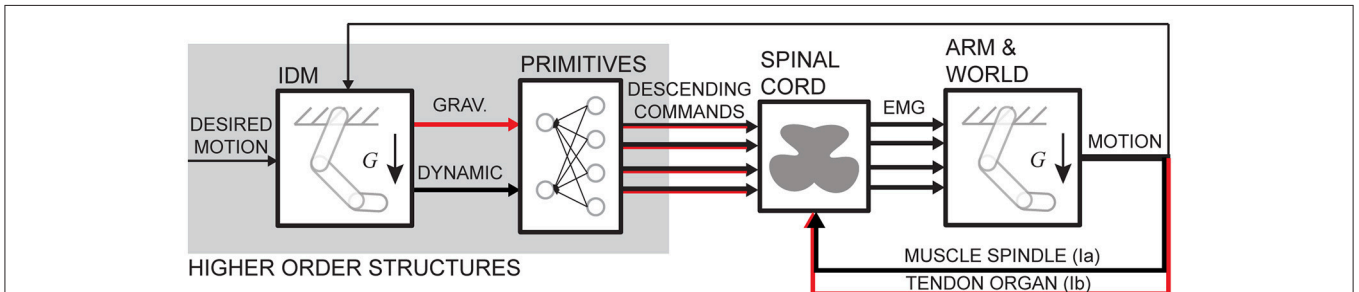
FIGURE 8 | Schematic of a motor control schema. Red arrows indicate signals potentially containing gravitational command components. Overlapping arrows indicate hybrid signals. IDM stands for inverse dynamic model, indicating a potential embedded limb dynamics.

may include full or partial compensation for gravity may constitute an anticipatory postural adjustment that accompanies movement that originates in the brainstem (Massion, 1992) or in the cerebellum (Sajdel-Sulkowska, 2013). Alternatively, or additionally, the gravitational command may be a spinal feedback response to changing gravitational load signaled by proprioceptors (**Figure 8**). The mechanism responsible for the feedback-driven compensation for gravity may be akin to positive force feedback during locomotion driven by afferent feedback from Golgi tendon organs to maintain load bearing (Pearson and Collins, 1993; Prochazka et al., 1997). These hypothetical neural commands, wherever they originate, would optimally combine (Chhabra and Jacobs, 2006; Gaveau et al., 2014, 2016; Vu et al., 2016) to drive the musculoskeletal system.

Unexpectedly, our results have shown that muscle activity waveforms consist of nearly equal contribution of gravitational and dynamic components. We found a linear relationship between the variance accounted for by the gravitational and dynamic components of EMG that was robust across subjects (**Figures 6**, **7**). This relationship is not a direct reflection of the relative contribution of torque components to muscle torque. This suggests that the musculoskeletal system, such as muscle moment arms around joints, muscle properties, and the composition of motor units, contribute to the scaling of muscle activity into appropriate moments (Gritsenko et al., 2016). Furthermore, we found that both the gravitational and dynamic components of EMG negatively correlated with the contribution of MD component to muscle torque. This means that the larger the contribution of MD to muscle torque, the smaller EMG variance is captured by the components of muscle torque. This may suggest that for more dynamic movements or when gravitational torques are smaller than dynamic torques, there is more co-contraction between muscles. Muscle co-contraction implies a common signal across several antagonistic muscles and is an important control strategy used to alter joint stiffness or whole arm impedance (Darainy et al., 2004; Damm and McIntyre, 2008). Furthermore, the dynamic component contributed about equally to EMG of most muscles (**Figure 4**). This suggests that the amount of co-contraction may be estimated from the relative contribution of the dynamic component to muscle torque.

Recent studies have provided evidence that gravity is optimally integrated into the neural control of movement (Crevecoeur et al., 2009; Wang and Dounskaia, 2016). This may be interpreted as contradictory to the idea of two command signals in EMG, gravitational for static and dynamic for phasic. The contradiction arises when the static component is thought to be eliminating the effect of gravity on the limb, while the optimal control takes advantage of gravity's assistive action instead of counteracting it (Wang and Dounskaia, 2016). Our data helps resolve this contradiction. The static gravitational component in EMG studied here does not necessarily completely counteract the force of gravity on the limb. At the same time, allowing gravity to passively move the limb does not mean that EMG in muscles

spanning the same or other joints would contain no gravity-related signals. For example, for downward movements, gravity could indeed substantially contribute to the movement reducing muscle action. However, the gravity component would still be present in active muscle torque and in EMG, because of the forces required to maintain arm posture against gravity at the beginning and/or at the end of movement. For our downward movement 9, the was significant gravity-related torque present at the shoulder (**Figure 2**). In fact, our segments usually do not move at linear acceleration of 9.8 m/s^2, which is the only case, other than in a microgravity environment, when no gravitational component in EMG would be expected. Therefore, the potential presence of a separate gravitational neural command does not contradict the fact that the CNS takes advantage of gravity to assist with movements.

CONCLUSIONS

In conclusion, our results have shown that gravitational and dynamic components of muscle torque represent significant amount of variance in muscle activity. This suggests that these torques may be used to estimate phasic and tonic components of muscle activity and may offer insight into neural control strategies.

AUTHOR CONTRIBUTIONS

EO contributed to the design of the study, subject recruitment, data collection, data analysis, and writing of the manuscript. BP contributed to the data collection and analysis, and to writing of the manuscript. VG contributed to the design of the study, analysis of data, and writing of the manuscript.

FUNDING

ACKNOWLEDGMENTS

SUPPLEMENTARY MATERIAL

The Supplementary Material for this article can be found online at: http://journal.frontiersin.org/article/10.3389/fnhum.2017.00474/full#supplementary-material

REFERENCES

d'Avella, A., Fernandez, L., Portone, A., and Lacquaniti, F. (2008). Modulation of phasic and tonic muscle synergies with reaching direction and speed. *J. Neurophysiol.* 100, 1433–1454. doi: 10.1152/jn.01377.2007

d'Avella, A., and Lacquaniti, F. (2013). Control of reaching movements by muscle synergy combinations. *Front. Comput. Neurosci.* 7:42. doi: 10.3389/fncom.2013.00042

Bastian, A. J., Martin, T. A., Keating, J. G., and Thach, W. T. (1996). Cerebellar ataxia: abnormal control of interaction torques across multiple joints. *J. Neurophysiol.* 76, 492–509.

Bizzi, E., Mussa Ivaldi, F., and Giszter, S. (1991). Computations underlying the execution of movement: a biological perspective. *Science* 253, 287–291. doi: 10.1126/science.1857964

Buneo, C. A., Soechting, J. F., and Flanders, M. (1994). Muscle activation patterns for reaching: the representation of distance and time. *J. Neurophysiol.* 71, 1546–1558.

Buneo, C. A., Soechting, J. F., and Flanders, M. (1997). Postural dependence of muscle actions: implications for neural control. *J. Neurosci.* 17, 2128–2142.

Chhabra, M., and Jacobs, R. A. (2006). Properties of synergies arising from a theory of optimal motor behavior. *Neural Comput.* 18, 2320–2342. doi: 10.1162/neco.2006.18.10.2320

Crevecoeur, F., Thonnard, J.-L., and Lefèvre, P. (2009). Optimal integration of gravity in trajectory planning of vertical pointing movements. *J. Neurophysiol.* 102, 786–796. doi: 10.1152/jn.00113.2009

Damm, L., and McIntyre, J. (2008). Physiological basis of limb-impedance modulation during free and constrained movements. *J. Neurophysiol.* 100, 2577–2588. doi: 10.1152/jn.90471.2008

Darainy, M., Malfait, N., Gribble, P. L., Towhidkhah, F., and Ostry, D. J. (2004). Learning to control arm stiffness under static conditions. *J. Neurophysiol.* 92, 3344–3350. doi: 10.1152/jn.00596.2004

Debicki, D. B., and Gribble, P. L. (2005). Persistence of inter-joint coupling during single-joint elbow flexions after shoulder fixation. *Exp. Brain Res.* 163, 252–257. doi: 10.1007/s00221-005-2229-6

Dounskaia, N. V., and Wang, W. (2014). A preferred pattern of joint coordination during arm movements with redundant degrees of freedom. *J. Neurophysiol.* 112, 1040–1053. doi: 10.1152/jn.00082.2014

Fisk, J., Lackner, J. R., and Dizio, P. (1993). Gravitoinertial force level influences arm movement control. *J. Neurophysiol.* 69, 504–511.

Flanders, M. (1991). Temporal patterns of muscle activation for arm movements in three-dimensional space. *J. Neurosci.* 11, 2680–2693.

Flanders, M., and Herrmann, U. (1992). Two components of muscle activation: scaling with the speed of arm movement. *J. Neurophysiol.* 67, 931–943.

Flanders, M., Pellegrini, J. J., and Geisler, S. D. (1996). Basic features of phasic activation for reaching in vertical planes. *Exp. Brain Res.* 110, 67–79. doi: 10.1007/BF00241376

Gaveau, J., Berret, B., Angelaki, D. E., and Papaxanthis, C. (2016). Direction-dependent arm kinematics reveal optimal integration of gravity cues. *Elife* 5, 763. doi: 10.7554/eLife.16394

Gaveau, J., Berret, B., Demougeot, L., Fadiga, L., Pozzo, T., and Papaxanthis, C. (2014). Energy-related optimal control accounts for gravitational load: comparing shoulder, elbow, and wrist rotations. *J. Neurophysiol.* 111, 4–16. doi: 10.1152/jn.01029.2012

Gaveau, J., Paizis, C., Berret, B., Pozzo, T., and Papaxanthis, C. (2011). Sensorimotor adaptation of point-to-point arm movements after spaceflight: the role of internal representation of gravity force in trajectory planning. *J. Neurophysiol.* 106, 620–629. doi: 10.1152/jn.00081.2011

Gentili, R., Cahouet, V., and Papaxanthis, C. (2007). Motor planning of arm movements is direction-dependent in the gravity field. *Neuroscience* 145, 20–32. doi: 10.1016/j.neuroscience.2006.11.035

Giszter, S. F., Mussa-Ivaldi, F. A., and Bizzi, E. (1993). Convergent force fields organized in the frog's spinal cord. *J. Neurosci.* 13, 467–491.

Gomi, H., and Kawato, M. (1997). Human arm stiffness and equilibrium-point trajectory during multi-joint movement. *Biol. Cybern.* 76, 163–171. doi: 10.1007/s004220050329

Gottlieb, G. L., Song, Q., Almeida, G. L., Hong, D. A., and Corcos, D. (1997). Directional control of planar human arm movement. *J. Neurophysiol.* 78, 2985–2998.

Gritsenko, V., Hardesty, R. L., Boots, M. T., and Yakovenko, S. (2016). Biomechanical constraints underlying motor primitives derived from the musculoskeletal anatomy of the human arm. *PLoS ONE* 11:e0164050. doi: 10.1371/journal.pone.0164050

Hollerbach, J. M., and Flash, T. (1982). Dynamic interactions between limb segments during planar arm movement. *Biol. Cybern.* 44, 67–77. doi: 10.1007/BF00353957

Lackner, J. R., and Dizio, P. (1994). Rapid adaptation to Coriolis force perturbations of arm trajectory. *J. Neurophysiol.* 72, 299–313.

Le Seac'h, A. B., and McIntyre, J. (2007). Multimodal reference frame for the planning of vertical arms movements. *Neurosci. Lett.* 423, 211–215. doi: 10.1016/j.neulet.2007.07.034

Manto, M. U., and Bosse, P. (2003). Directional tuning of speed-related activation for reaching in the vertical plane in cerebellar ataxia. *Neurol. Res.* 25, 434–444. doi: 10.1179/016164103101201715

Massion, J. (1992). Movement, posture and equilibrium: interaction and coordination. *Prog. Neurobiol.* 38, 35–56. doi: 10.1016/0301-0082(92)90034-C

Mussa Ivaldi, F. (1999). Modular features of motor control and learning. *Curr. Opin. Neurobiol.* 9, 713–717. doi: 10.1016/S0959-4388(99)00029-X

Mussa Ivaldi, F., and Bizzi, E. (2000). Motor learning through the combination of primitives. *Philos. Trans. R. Soc. Lond. B.* 355, 1755–1769. doi: 10.1098/rstb.2000.0733

Papaxanthis, C., Pozzo, T., and McIntyre, J. (2005). Kinematic and dynamic processes for the control of pointing movements in humans revealed by short-term exposure to microgravity. *Neurosci* 135, 371–383. doi: 10.1016/j.neuroscience.2005.06.063

Papaxanthis, C., Pozzo, T., Popov, K. E., and McIntyre, J. (1998). Hand trajectories of vertical arm movements in one-G and zero-G environments. Evidence for a central representation of gravitational force. *Exp. Brain Res.* 120, 496–502. doi: 10.1007/s002210050423

Pearson, K. G., and Collins, D. F. (1993). Reversal of the influence of group Ib afferents from plantaris on activity in medial gastrocnemius muscle during locomotor activity. *J. Neurophysiol.* 70, 1009–1017.

Pozzo, T., Papaxanthis, C., Stapley, P., and Berthoz, A. (1998). The sensorimotor and cognitive integration of gravity. *Brain Res. Brain Res. Rev.* 28, 92–101. doi: 10.1016/S0165-0173(98)00030-7

Prochazka, A., Gillard, D. M., and Bennett, D. J. (1997). Positive force feedback control of muscles. *J. Neurophysiol.* 77, 3226–3236.

Robertson, G., Caldwell, G., Hamill, J., Kamen, G., and Whittlesey, S. (2013). *Research Methods in Biomechanics, 2E.* Human Kinetics.

Rousseau, C., Papaxanthis, C., Gaveau, J., Pozzo, T., and White, O. (2016). Initial information prior to movement onset influences kinematics of upward arm pointing movements. *J. Neurophysiol.* 116, 1673–1683. doi: 10.1152/jn.00616.2015

Russo, M., D'Andola, M., Portone, A., Lacquaniti, F., and d'Avella, A. (2014). Dimensionality of joint torques and muscle patterns for reaching. *Front. Comput. Neurosci.* 8:24. doi: 10.3389/fncom.2014.00024

Sabes, P. N. (2000). The planning and control of reaching movements. *Curr. Opin. Neurobiol.* 10, 740–746. doi: 10.1016/S0959-4388(00)00149-5

Sainburg, R. L., Ghez, C., and Kalakanis, D. (1999). Intersegmental dynamics are controlled by sequential anticipatory, error correction, and postural mechanisms. *J. Neurophysiol.* 81, 1045–1056.

Sainburg, R. L., Ghilardi, M., Poizner, H., and Ghez, C. (1995). Control of limb dynamics in normal subjects and patients without proprioception. *J. Neurophysiol.* 73, 820–835.

Sajdel-Sulkowska, D. E. M. (2013). "Cerebellum and gravity: altered earth's gravity perception under pathological conditions and response to altered gravity in space," in *Handbook of the Cerebellum and Cerebellar Disorders*, eds M. Manto, D. L. Gruol, J. D. Schmahmann, N. Koibuchi, and F. Rossi (Dordrecht: Springer Netherlands), 1241–1255.

Shabbott, B. A., and Sainburg, R. L. (2008). Differentiating between two models of motor lateralization. *J. Neurophysiol.* 100, 565–575. doi: 10.1152/jn.90349.2008

Shadmehr, R., and Mussa Ivaldi, F. (1994). Adaptive representation of dynamics during learning of a motor task. *J. Neurosci.* 14, 3208–3224.

Talkington, W. J., Pollard, B. S., Olesh, E. V., and Gritsenko, V. (2015). Multifunctional setup for studying human motor control using transcranial magnetic stimulation, electromyography, motion capture, and virtual reality. *J. Vis. Exp.* e52906. doi: 10.3791/52906

Thomas, J. S., Corcos, D. M., and Hasan, Z. (2005). Kinematic and kinetic constraints on arm, trunk, and leg segments in target-reaching movements. *J. Neurophysiol.* 93, 352–364. doi: 10.1152/jn.00582.2004

Vu, V. H., Isableu, B., and Berret, B. (2016). On the nature of motor planning variables during arm pointing movement: compositeness and speed dependence. *Neuroscience* 328, 127–146. doi: 10.1016/j.neuroscience.2016.04.027

Wang, W., and Dounskaia, N. V. (2016). Neural control of arm movements reveals a tendency to use gravity to simplify joint coordination rather than to decrease muscle effort. *Neuroscience* 339, 418–432. doi: 10.1016/j.neuroscience.2016.10.009

Weiss, E. J., and Flanders, M. (2004). Muscular and postural synergies of the human hand. *J. Neurophysiol.* 92, 523–535. doi: 10.1152/jn.01265.2003

Winter, D. A. (2009). *Biomechanics and Motor Control of Human Movement.* 4 Edn, Hoboken, NJ: John Wiley & Sons.

Wolpert, D. M., and Kawato, M. (1998). Multiple paired forward and inverse models for motor control. *Neural Netw.* 11, 1317–1329. doi: 10.1016/S0893-6080(98)00066-5